atmosphere

MDPI

Article

The Impact of Climate Change on Solar Radiation and Photovoltaic Energy Yields in China

Yaping Hua [1,*], Mingbang Wei [1], Jun Yuan [1], Wei He [1], Long Chen [1] and Yang Gao [2,*]

[1] Gansu Natural Energy Research Institute, Gansu Academy of Sciences, Lanzhou 730046, China
[2] Key Research Institute of Yellow River Civilization and Sustainable Development, Henan University, Zhengzhou 450001, China
* Correspondence: butty2001@163.com (Y.H.); gaoyang@henu.edu.cn (Y.G.)

Abstract: Solar photovoltaics is a direct use of solar resources to generate electricity, which is one of the most important renewable energy application approaches. Regional PV output could be affected by the regional patterns of temperature and irradiance, which are impacted by climate change. This study examines the impact of climate change on the energy yields from solar PV across China in the future under the medium-emission scenario (SSP245) and high-emission scenario (SSP585) by calculating PV potential using the data of solar radiation on a tilted surface and temperature. Generally, under the SSP245 scenario, solar radiation increased by 0.8% and 2.15%, and PV energy yields increased by 0.28% and 1.21% in 2020–2060 and 2061–2099, respectively; under the SSP585 scenario, solar radiation increased by 0.73% and 1.35%, and PV energy yields increased by 0.04% and −1.21% in 2020–2060 and 2061–2099, respectively. Under both scenarios, PV energy potential showed an obvious increase in southeast and central China and a significant decrease in northwest China, Tibet, and Inner Mongolia. Therefore, it is suggested that under the medium-emission scenario, climate change could increase the PV energy potential, while under the high-emission scenario, it could inhibit the PV energy potential in China.

Keywords: climate change; CMIP6; solar photovoltaics; energy yield potential; solar radiation; temperature; SSP245; SSP585

Citation: Hua, Y.; Wei, M.; Yuan, J.; He, W.; Chen, L.; Gao, Y. The Impact of Climate Change on Solar Radiation and Photovoltaic Energy Yields in China. *Atmosphere* **2024**, *15*, 939. https://doi.org/10.3390/atmos15080939

Academic Editors: Hamid Pouran, Yong Sheng, Ahmet Duran Şahin and Mustafa Kemal Kaymak

Received: 4 July 2024
Revised: 29 July 2024
Accepted: 1 August 2024
Published: 5 August 2024

1. Introduction

The solar photovoltaic power system is a direct use of solar resources to generate electricity, which has become one of the most important renewable energy application approaches. At the end of 2022, there was 1185 GW of annually installed capacity across the world [1]. Meanwhile, the earth's climate will have significant changes in coming decades worldwide, due to anthropogenic emissions. Global solar radiation, ambient temperature, wind speed, snow, dust, and so on would influence the photovoltaic energy yields [2]. Among these factors, global solar radiation and ambient temperature are the most important factors. Photovoltaic output has an approximately proportional response to global solar radiation, except for low-level values, and a near linear response to cell temperature related to ambient temperature with a negative gradient [3]. The changes in air temperature are an acknowledged fact across the world. In contrast, solar radiation is considered a constant. Nevertheless, from long-term observation, solar radiation is undergoing significant multi-decadal variations [2,4]. There is "global dimming" (solar radiation decreased from 1950s to 1980s) and "global brightening" (solar radiation has increased since the late 1980s) from worldwide observation networks, which is in accordance with anthropogenic activities [5,6]. The regional PV output could be affected by the regional patterns of temperature and irradiance, which are impacted by climate change [3]. The sensitivity of potential photovoltaic energy to future climate change is a major concern for policy makers before large-scale investment in photovoltaic systems.

The Coupled Model Intercomparison Project that began in 1995 under the auspices of the World Climate Research Programme (WCRP) is now in its sixth phase (CMIP6). CMIP6 coordinates somewhat independent model intercomparison activities, and their experiments have adopted a common infrastructure for collecting, organizing, and distributing output from models performing common sets of experiments. There are a few studies on the estimation of the PV energy yields under different climate change scenarios. The power output of photovoltaics under RCP8.5 scenarios was projected across the world during the time period of 2006–2049, based on CMIP5 data, and it was found that there is a significant decrease in photovoltaic power output in large parts of the world, except for southeast China, southeast North America, and a large of Europe, where the output shows positive change trends, due to their increase in clear sky radiation and decrease in cloud cover [2]. Meanwhile, the PV potentials in Europe were investigated by the researchers [4,7–9]. Other scholars using CMIP6 data projected the future yields of PV in the world under low-, medium-, and high-emission scenarios and discovered that the output of PV showed a 6~10% decrease (refer to 1981–2014 climatology) in China [10]. Additionally, scholars investigated the projection of PV power potential in the context of climate change in West Africa and Brazil, based on CMIP6 data [11,12]. There are also a few studies focused on the projection of China's PV power potential in the future in the context of climate change [13–16]. Among them, it was found that PV power output will decrease in the northwest of China and increase eastern China [15]. It was demonstrated that the annual PV power generation in the northern and Tibet regions will decrease, while in the southern and central regions, it will increase [16]. In addition, China's solar energy potential changes under different emission scenarios were assessed, and it was found that solar energy potential will increase as a result of emission reduction [17]. Although the above studies investigated China' s PV power potential to some extent, there are few studies on the projected energy yields from photovoltaics, which can more directly see the electricity generated from photovoltaics. Moreover, most researchers calculated PV output using horizontal solar radiation without consideration the tilted angle of photovoltaic panels in real life. Although some researchers calculated the tilted angles in Europe and China using a simple linear regression equation [18,19], according to other studies [20,21], the real process of solar radiation falling to the PV panels is not considered, which may lead to error to some extent.

This study considered the solar radiation falling on tilted PV panels and the electricity generated from PV to examine the impact of climate change on solar radiation and energy yields from PV across China under different emission scenarios, which would provide a more scientific theoretical basis for the Chinese government to develop the photovoltaic industry. The periods can be divided into the referenced historical period (1990–2010), the near future (2020–2060), and the far future (2061–2099). Firstly, the optimum tilted angles of PV panels across China were calculated. Secondly, the changes in solar radiation and temperature were analyzed. Then, the energy yields from PV were projected through Crook's model [3], based on CMIP6 data. Finally, according to the analyzed results, the discussion was conducted by comparing the results with the studies by other researchers, and the conclusion was drawn at the end.

2. Data and Methodology

2.1. Data

In this part, the Coupled Model Intercomparison Project Phase 6 is introduced. The PV panels' optimum tilted angle calculation and empirical models for photovoltaic output prediction are introduced as well.

CMIP6 proposes new projected scenarios using six integrated assessment models (IAMs), based on different shared socioeconomic pathways (SSPs) and the latest anthropogenic emissions trends, which are listed as sub-programs of the CMIP6 model comparison, called Scenario Models Compare Plans (ScenarioMIP). The climate scenarios for ScenarioMIP are rectangular combinations of different shared socioeconomic pathways

(SSPs) and radiative forcing. SSP describes the possible development of society in the future without the influence of climate change or climate policy [22]. This study selected the SSP245 and SSP585 scenarios, which represent medium and high emissions, respectively.

In this research, the global climate models (GCMs) of monthly surface downwelling shortwave radiation (rsds) (W/m^2), near-surface air temperature (2 m) (tas) (°C), and surface diffuse downwelling shortwave flux in air (rsdsdiff) (W/m^2) were obtained from CMIP6. All the available models of data were downloaded and unified into a resolution of 1° × 1° using the bilinear interpolation method. In order to verify that the CMIP6 data were appropriate for China, the tas and rsds data from GCMs were compared with China's total solar radiation data (1981–2010), which are also the grid data based on instrumental measurement [23] and the 0.5° × 0.5° grid point temperature data from China's Meteorological Network in the historical period, respectively. The correlation (COR), root mean square error (RMSE), and standard deviation (SD) were used to evaluate data quality. The COR, RMSE, and SD ranges for tas were 0.805~0.994, 1.307~8.637 °C, and 1.918~9.798 °C, respectively. The COR, RMSE, and SD ranges for rsds were 0.926~0.986, 8.601~18.552 W/m^2, and 43.832~55.328 W/m^2, respectively. There was only one model available (CESM2-WACCM) for rsdsdiff from CMIP6, which was used together with tas and rsds for calculating the optimum tilted angles of photovoltaic panels in China. After a comprehensive consideration of three error indicators, consequently, the following models' data were selected for tas, rsds, and rsdsdiff, as shown in Table 1. The mean values of the selected models were applied in the simulation.

Table 1. The selected CMIP6 models for tas, rsds, and rsdsdiff.

GCMs	Model Name	Country	Units	Resolution (km)
tas	ACCESS-CM2	Australia	CSIRO-BOM	100
	GISS-E2-1-H	America	GISS	50
	GISS-E2-1-G	America	GISS	250
	KIOST-ESM	Korea	KIOST	100
	MRI-ESM2-0	Japan	MRI	60
	MPI-ESM-1-2-HAM	Germany	MPI-M	110
	NorESM2-LM	Norway	NCC	250
rsds	BCC-CSM2-MR	China	BCC	110
	CCCR-IITM-ESM	India	IITM	70
	KACE-1-0-G	Korea	KIAPS	100
	MPI-ESM1-2-LR	Germany	MPI-M	110
	MPI-ESM1-2-HR	Germany	MPI-M	50
	NorESM2-MM	Norway	NCC	110
rsdsdiff	CESM2-WACCM	USA	NCCR	100

2.2. Methodology

The following part will discuss the methodology of calculating PV energy output, as shown in Figure 1.

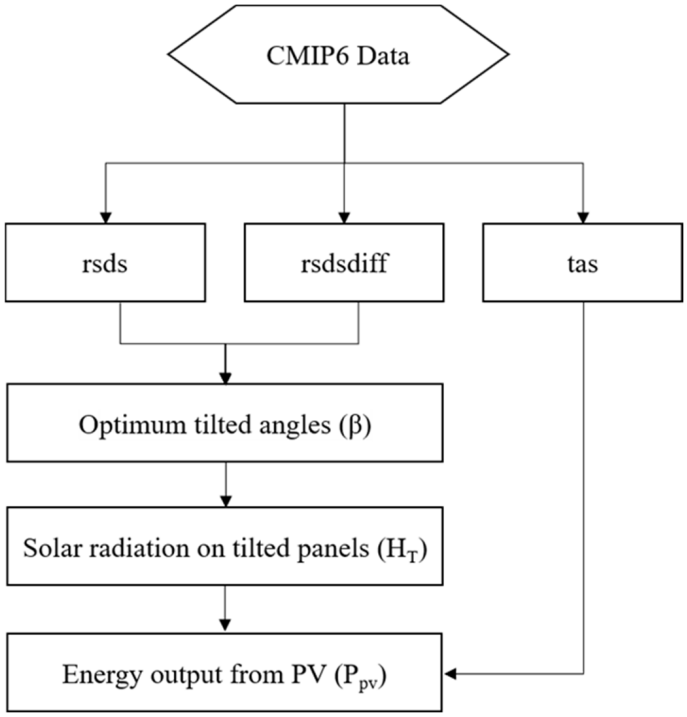

Figure 1. The flowchart of PV energy output.

2.2.1. Calculation of Solar Radiation on a Tilted Surface at the Optimum Tilted Angle

According to the studies on the optimum tilted angle of solar panels in China, there are several existing mathematic models to calculate solar irradiance on the tilted surface via available horizontal solar irradiance data. Herein, the sky isotropic model by Liu and Jordan [24] and sky anisotropy models by Hay [25] were selected in this study because they are classical and theoretical models and widely used in the world. The optimum tilted angle and solar radiation on the tilted surface would be the mean values of these two models, according to the scholars' research [26].

2.2.2. Projection of the Energy Yields from Solar PV

This study applied Crook et al.'s [3] empirical model to project the energy yield from PV in historical and future periods in the context of climate change (under SSP245 and SSP585 scenarios). The calculations were as follows:

$$\frac{\eta_{cell}}{\eta_{ref}} = 1 - \alpha(T_{cell} - T_{ref}) + \gamma \log_{10} H_T \quad (1)$$

where η_{ref} is the reference efficiency, normally $\eta_{ref} = 0.12$ [27], and α and γ are the coefficients of temperature and irradiance that are determined by the material and structure of the cell. T_{cell} and T_{ref} are the cell and reference temperatures, respectively, while γ represents the characteristics of the decreases in silicon PV efficiency at low-light levels [27–29]. In this study, $\alpha = 0.0045$ and $\gamma = 0.1$ were used for calculation, typical for monocrystalline silicon cells, and $T_{ref} = 25\ ^{\circ}C$. Meanwhile, the temperature of the cells can be calculated as follows:

$$T_{cell} = c_1 + c_2 T + c_3 H_T \quad (2)$$

where T is the ambient temperature (°C), and the coefficients are used for calculation, according to Lasiner and Ang [30]:

$$C_1 = -3.75\ ^{\circ}C,\ C_2 = 1.14,\ C_3 = 0.0175\ ^{\circ}C\ m^2/W \quad (3)$$

Moreover, the power output of photovoltaics can be calculated as follows:

$$P_{pv} = H_T \eta_{cell}$$

where H_T represents the solar radiation on the tilted PV panels set at the yearly optimum tilted angle (β).

P_{PV} is the average power output of the monthly representative day for 24 h (W/m^2); it can be converted into the yearly energy (kWh/m^2) from P_{PV} using the following equation:

$$E = \sum_{1}^{12} P_{pv} \times S_0 \times 3600 \times N \quad (4)$$

Here, N is the representative day of each month in a year proposed by Klein [31], as shown in Table 2.

Table 2. The representative day of each month in a year.

Month	January	February	March	April	May	June	July	August	September	October	November	December
Date	17	16	16	15	15	11	17	16	15	15	14	10
N	17	47	75	105	135	162	198	228	258	288	318	344

S_0 represents the sunlight hours, and it can be calculated by the following equation:

$$S_0 = \frac{2}{15} \arccos(-\tan\varphi \tan\delta) \quad (5)$$

where φ is the latitude, and δ is the solar declination, which can be defined by the following equation:

$$\delta = 23.45 \sin(360(284 + N)/365) \quad (6)$$

3. Results

3.1. The Spatial Distribution of Yearly Optimum Tilted Angles (β) in China

As shown in Figure 2, overall, the yearly optimum tilted angles are high in the north and low in the south of China. When the latitude decreases, the optimum tilted angle decreases as well. The highest values (≥45°) are in the northeast part of China, including Heilongjiang, the northwest part of the Jilin province, and the northeast of the Inner Mongolia Autonomous Prefecture. The lowest values (≤20°) are in Hainan and the south parts of the Guangxi, Guangdong, and Fujian provinces. However, China's photovoltaic installations are mainly distributed in the northwest part of China. The optimum tilted angles range from 35° to 42°, which is consistent with their latitude (37°~50°). It can be seen that the optimum tilted angle from the models is slightly lower than its latitude.

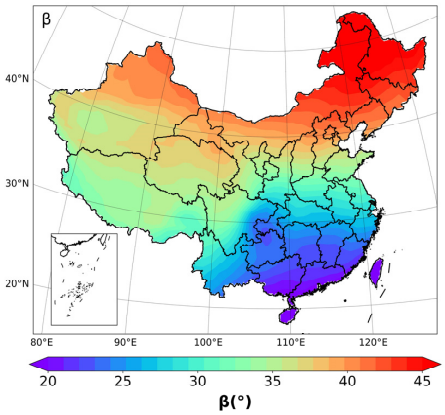

Figure 2. The yearly optimum tilted angles of photovoltaic panels in China.

3.2. Annual Energy Output of Photovoltaics in the Historical Period (1990–2010)

As shown in Figure 3a, during the time period of 1990–2010, the highest values of annual solar radiation on the horizontal surface (rsds) (MJ/m^2) are distributed in eastern and central Tibet, and the sub-highest values are distributed in parts of the Qinhai, Gansu, and Xinjiang provinces, while the lowest values are distributed in the southwest of Tibet and the eastern and central parts of China. It can be seen from Figure 3b that generally, the solar radiation on a tilted surface in northern China is higher than that in southern China because of high amounts of diffuse solar radiation in the southern part of China. Referring to near-surface air temperature (tas), as shown in Figure 3c, during the years of 1990–2010, the annual average low values of near-surface air temperature are distributed in the Qinghai–Tibet Plateau (about 0 °C), while the high-value areas are in the southeastern part of China (15 °C). How do the solar radiation and near-surface air temperature affect the energy output of the photovoltaics? Figure 3d illustrates that the spatial distribution of the annual average photovoltaic energy generation is positively correlated with solar radiation, especially solar radiation on a tilted surface, while it is negatively correlated with near-surface air temperature. Furthermore, it seems that solar radiation is the main factor affecting photovoltaic energy generation, compared with near-surface air temperature. The national annual average value of energy generated from photovoltaics is 299.55 kWh/(m^2·year). The highest value is in Tibet, reaching 400 kWh/(m^2·year), while the lowest value is in the northernmost part of northeastern China, with only about 200 kWh/(m^2·year). The annual PV energy yield in the northwest of China, which is the preferred site selection of the utility-scaled photovoltaic installations, due to its richness in solar radiation and huge land areas, ranges from 300~400 kWh/(m^2·year).

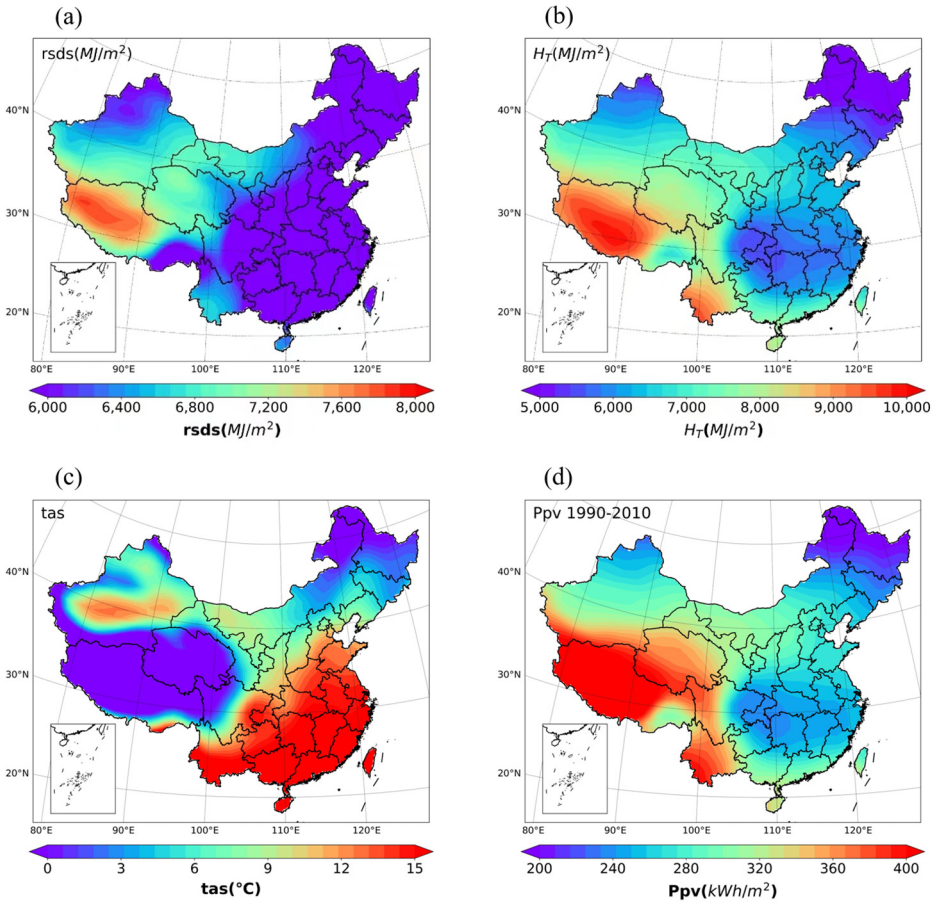

Figure 3. The spatial distributions of rads, H_T, tas, and P_{pv} during the time period of 1990–2010.

3.3. Projection of Changes in Solar Radiation

The solar radiation on the inclined surface is calculated from the solar radiation on the horizontal surface, and they are positively correlated. Herein, the changes in solar radiation on the horizontal plane are discussed to reflect the future trend of solar radiation. When calculating the photovoltaic energy generation, the values of solar radiation on the inclined surface are used.

As shown in Figure 4a,b, under the medium-emission scenario (SSP245), from a national perspective, the annual average change rate of solar radiation on the horizontal surface during the years of 2020–2060 is 0.8% (48.68 MJ/m^2), ranging from −1% to 5% (−60 MJ/m^2 to 180 MJ/m^2), compared with the historical period (1990–2020). The change rate of solar radiation in northern China is relatively small, ranging from −1% to 1%, while the change rate in southern China is significantly higher than that in the north, especially in western Guizhou, northern Guangxi, southeastern Hubei, southern Anhui, Hunan, and most of the areas of Jiangxi and Zhejiang, where the change rate of solar radiation is as high as 4%, with a variation of 180 MJ/m^2. In the same way, under the high-emission scenario (SSP585), as shown in Figure 4c,d, the average change rate is 0.73% (44.1 MJ/m^2) in China. In northern China, the change rate is $\leq \pm 1.5\%$, with a variation of ± 80 MJ/m^2, while the largest change rate in southern China is about 5%, with a change of 260 MJ/m^2. Compared with the SSP245 scenario, the obvious difference is that the area with a large change rate in the south shrinks significantly, only in northeastern Jiangxi, northern Fujian, and southwestern Zhejiang, where the change rate of solar radiation reaches 5%.

As shown in Figure 4e,f, during the time period of 2061–2099, under the SSP245 scenario, compared with that of 2020–2060, the obvious difference is that the areas of the central and southeastern regions of China with a solar radiation increase have expanded. The average change rate of solar radiation in China is 2.15% (130.04 MJ/m^2). The highest change rate is 10% (300 MJ/m^2), referred to in the historical period. In the same way, under the SSP585 scenario, as shown in Figure 4g,h, the average change rate is 1.35% (81.55 MJ/m^2). The ranges of the change rate and variation referred to in the historical period are about −2~10% and −120 MJ/m^2~300 MJ/m^2, respectively, which are greater than that of the 2020–2060 period overall. Therefore, it is necessary to note that during the years of 2020–2099, under both emission scenarios, the overall trend of solar radiation in China increases. However, there are decreases in solar radiation in the northwest part of China (including most of Gansu, Qinghai, and Xinjiang provinces), parts of the Tibetan Plateau, and west of Inner Mongolia. Increases in solar radiation are observed in other regions of China, as shown in Table 3.

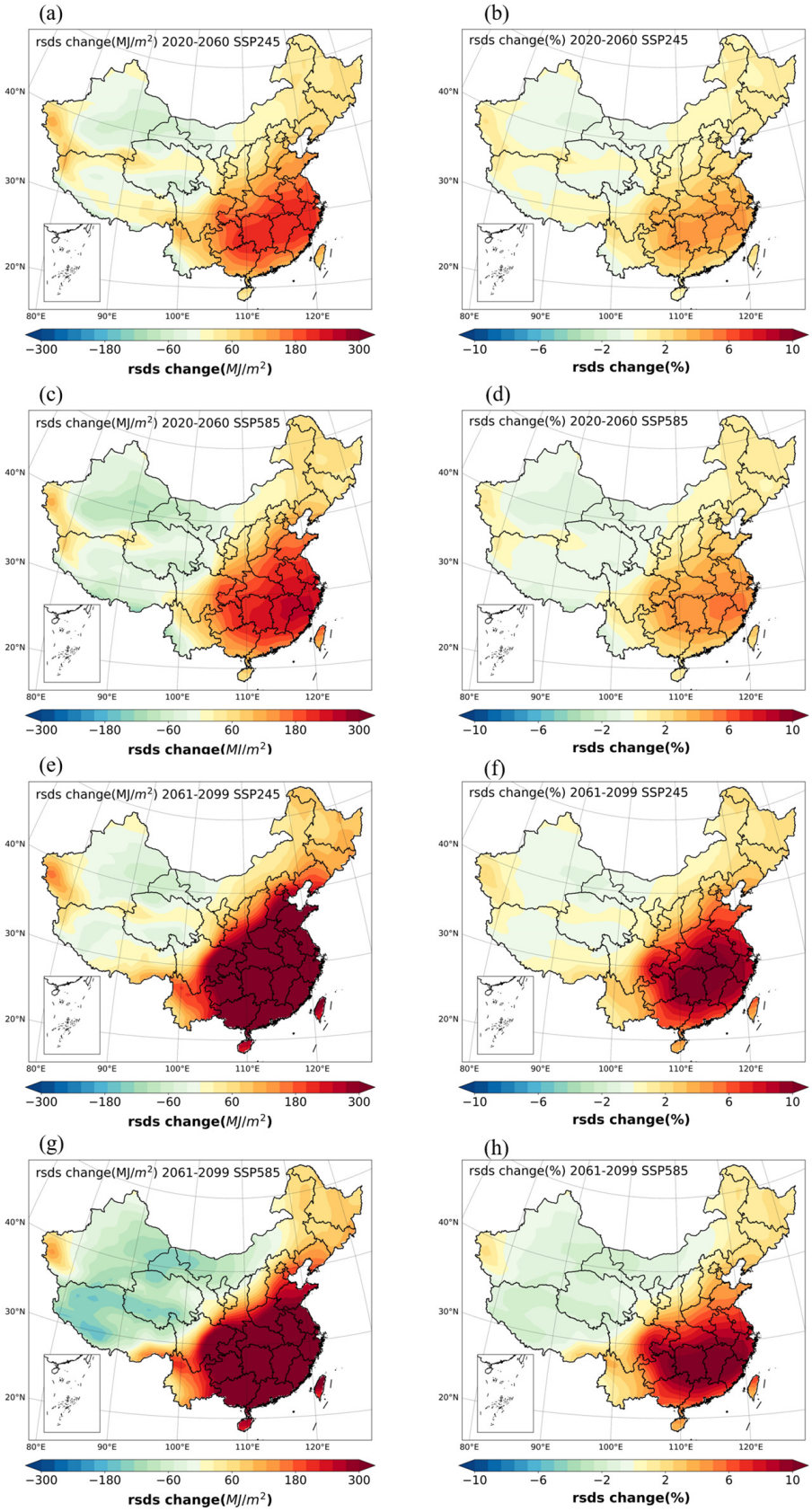

Figure 4. The distribution of solar radiation changes during the time period of 2020–2099 in the SSP245 and SSP585 scenarios.

Table 3. The change rates of solar radiation in significant regions.

Variable	Scenario	Period	China	Northwest	Tibet	Inner Mongolia	Southeast	Central
rsds change (%)	ssp245	2020–2060	0.80	−0.06	0.05	0.51	3.58	3.66
		2061–2099	2.15	0.28	0.03	1.93	8.67	9.35
	ssp585	2020–2060	0.73	−0.38	−0.37	0.67	4.33	4.28
		2061–2099	1.35	−0.60	−1.29	0.48	8.27	8.61

3.4. Projection of the Changes in Near-Surface Air Temperature

Considering the annual average temperature would be minus in some regions (Tibetan Plateau), which would lead to the minus value of the temperature change rate, herein, only the temperature change is analyzed in this part.

During the years of 2020–2060, as shown in Figure 5a, under the SSP245 scenario, for the whole country, the annual average near-surface air temperature will increase by 1.53 °C. It will increase by nearly 1.6 °C in most parts of northern China, while it will increase by 1.3 °C in southern and central China. Meanwhile, as shown in Figure 5b, under the SSP585 scenario, the annual average near-surface air temperature shows a more obvious increasing trend than that of SSP245. Overall, the average temperature increase in China is 1.82 °C. In most of the regions, the temperature will exceed 1.6 °C, except for most of Yunnan, Sichuan, Guizhou, and a very few areas in southern Tibet. Furthermore, the western part of Tibet, most of Xinjiang, the zone where Gansu and Qinghai meet, and very few regions in northeastern China will experience a temperature rise of more than 2 °C. Therefore, under the high-emission scenario, the temperature increase is greater than that in the low-emission scenario, and the areas with a relatively large increase in temperature show a significantly expanded tendency.

From 2061 to 2099, as shown in Figure 5c, under the SSP245 scenario, for the whole country, the annual average temperature will increase by 2.66 °C. In northern China, it is generally greater than 2.66 °C, while in southern China, it is greater than 2 °C. In eastern Tibet and some of the southern and northern areas of Xinjiang, the temperature rises by about 3.6 °C. Thus, the annual average temperature is higher than that of 2020–2060, which implies that even under the same emission scenario, the trend of global warming is gradually increasing. Under the SSP585 scenario, as shown in Figure 5d, overall, the annual average temperature rises by 4.4 °C. In most parts of northern China, the temperature is greater than 4.6 °C, and in some parts of Tibet, Gansu, Xinjiang, Inner Mongolia, and northeast China, the temperature rise exceeds 4.8 °C, while in southern China, the temperature rise also exceeds 3.8 °C. Therefore, the largest temperature increase occurs under the SSP585 scenario during the years of 2061–2099. Thus, the increase in temperature becomes progressively intense as time goes on and intensifies emissions, as shown in Table 4.

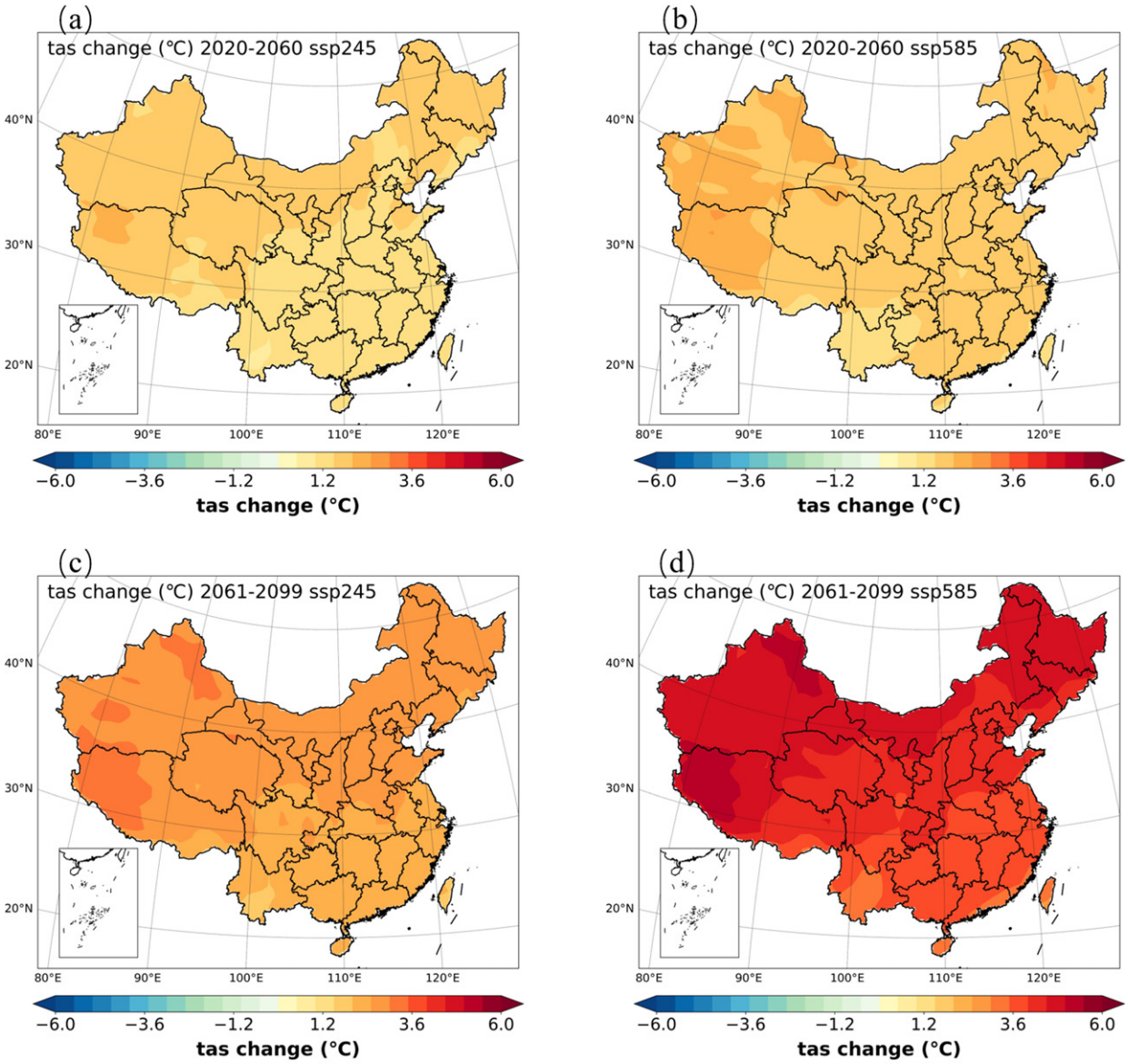

Figure 5. The distribution of the changes in temperature during the time period of 2020–2099 in the SSP245 and SSP585 scenarios.

Table 4. The changes in temperature in significant regions.

Variable	Scenario	Period	China	Northwest	Tibet	Inner Mongolia	Southeast	Central
tas changes	ssp245	2020–2060	1.53	1.67	1.67	1.53	1.32	1.28
		2061–2099	2.65	2.86	2.79	2.68	2.34	2.41
	ssp585	2020–2060	1.82	1.97	1.97	1.81	1.58	1.58
		2061–2099	4.39	4.68	4.58	4.44	3.73	3.89

3.5. Projection of Changes in PV Energy Output in the Future

Under both scenarios, from the national perspective, the annual average PV energy generation is not much different, compared with that of the historical period (1990–2020). As shown in Figure 6a,b, from 2020 to 2060, under the SSP245 scenario, the average change rate of PV energy output is 0.27%. The obvious changes are in the central and southeastern parts of China, including most of the Hunan and Jiangxi provinces and parts of the Hubei, Anhui, Zhejiang, and Fujian provinces, in which the annual average change rates and change values of photovoltaic energy generation are between 6~10% and 8~12 kWh/m^2, respectively. The change rate of the other regions varies from 0~±2% (0~±4 kWh/m^2). Meanwhile, under the high-emission scenario, as shown in Figure 6c,d, the average change rate of PV energy generation is 0.04%. The change rate in southern China, including the whole Jiangxi province, ranges from 3% to 6%, with corresponding changes of 6 kWh/m^2 to 12 kWh/m^2. In other regions of China, the change rate varies from 0~±2% (0~±4 kWh/m^2). Attention should be paid to the fact that under the high-emission scenario, the decrease in annual average photovoltaic energy generation in most of the northern parts of China (especially in the northwest of China) is slightly greater than that of the low-emission scenario.

In the same way, under both emission scenarios, during the years of 2061–2099, the average change rate of PV energy yields is about 1.21%. The decreases occur in the northwest regions (including Gansu, Qinghai, Xinjiang, and Ningxia), Tibetan Plateau, and Inner Mongolia. As shown in Figure 6e,f, under the SSP245 scenario, the obvious increases are still observed in some parts of central and southeastern China, with a change rate of 6~10% (12~20 kWh/m^2). In other regions of China, the change rate of the photovoltaic energy yield is about −2~6% (−4~12 kWh/m^2). Meanwhile, as shown in Figure 6g,h, under the SSP585 scenario, the average change rate of PV energy generation is −0.33%. The most obvious increases occur in southeastern and central China, with a change rate of 6~10% (6~20 kWh/m^2), while the change rate in other regions is 0~±6% (0~±12 kWh/m^2). Compared with the SSP245 scenario, the areas with the obvious increase in energy yield from photovoltaics slightly decreases.

Thus, under the low-emission scenario, from 2020 to 2099, as the time goes on, the change rate of the PV energy yield increases, which means the positive effect from increased solar radiation outweighs the negative temperature effect. Nevertheless, under the high-emission scenario, the change rate of the PV energy yield decreases gradually, since the effect of the large increase in temperature outweighs the effect resulting from the solar radiation increase. Furthermore, there are imbalance changes that occur in different regions of China under both scenarios. Generally, there are obvious increases in southeastern and central China, while decreases are observed in northwestern China, the Tibetan Plateau, and Inner Mongolia, as shown in Table 5.

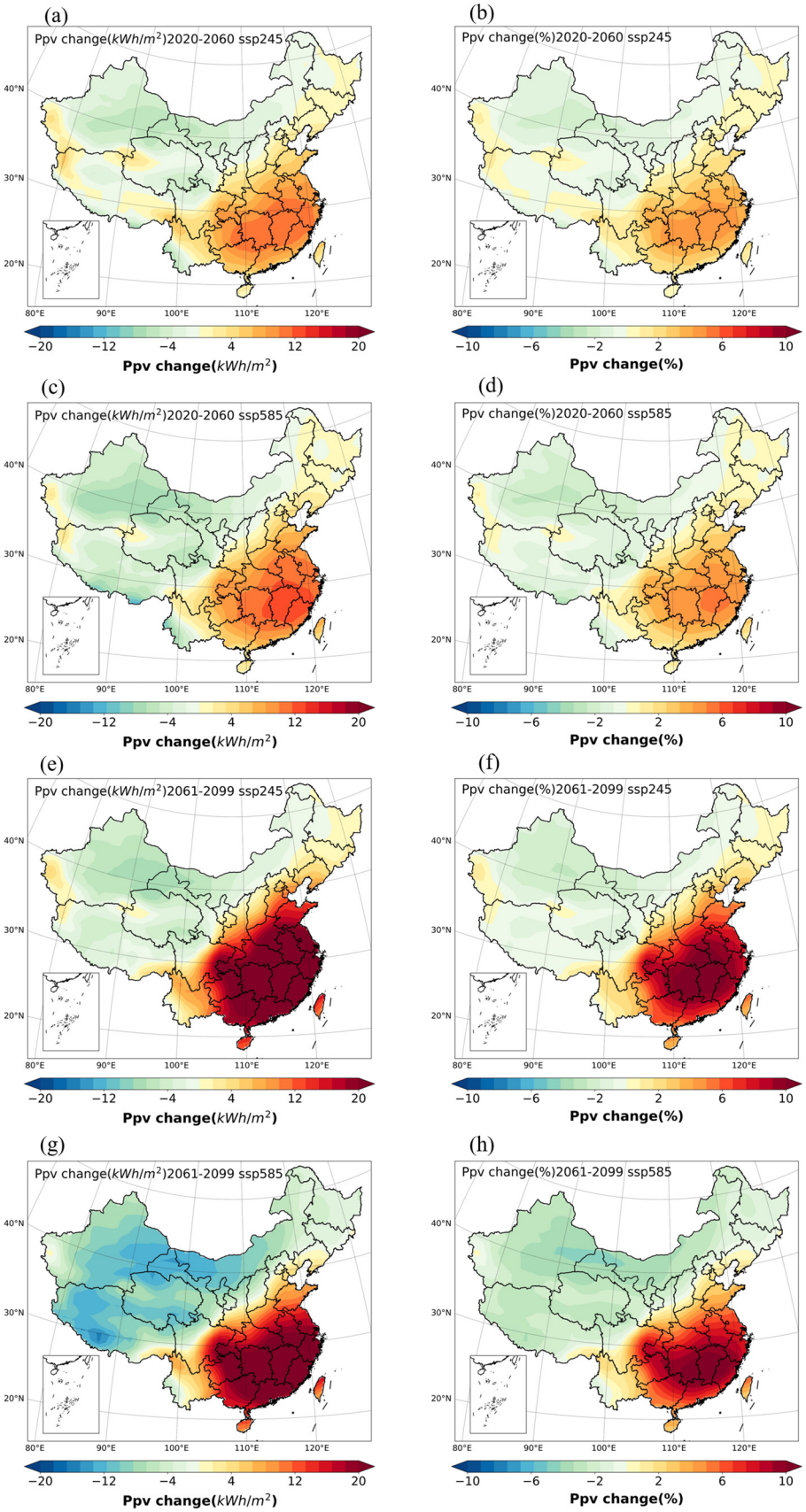

Figure 6. The distribution of PV energy output changes during the time period of 2020–2099 in the SSP245 and SSP585 scenarios.

Table 5. The change rates of PV energy output in significant regions.

Variable	Scenario	Period	China	Northwest	Tibet	Inner Mongolia	Southeast	Central
P_{pv} change (%)	ssp245	2020–2060	0.28	−0.85	−0.19	−0.30	3.51	3.66
		2061–2099	1.21	−1.05	−0.61	0.64	8.56	9.25
	ssp585	2020–2060	0.04	−1.34	−0.88	−0.17	4.15	4.16
		2061–2099	−0.33	−2.71	−2.40	−1.67	7.67	7.84

4. Discussion

In this study, under both emission scenarios, the overall trend of China's PV energy output does not change much, compared with the referenced period (1990–2010). Nevertheless, the changes show spatial and temporal imbalances in China. Spatially, there are obvious increases in southeastern and central China and significant decreases in northwest China, Tibetan Plateau, and Inner Mongolia under both the SSP245 and SSP585 scenarios. These results are partly consistent with other scholars' studies in the following ways. There are increases and decreases in PV potential occurring in the southeast of China and the Tibetan Plateau, respectively, under the RCP 8.5 scenario between 2006 and 2019 [6], which agrees with our study. Moreover, there is an increase in central China and a decrease in the Tibetan plateau, with a change of ±3 kWh/(m^2·year) under the RCP 8.5 scenario in 2006–2100 [32]. This is numerically different from this study, in which there are increases and decreases in central China and Tibet, with changes of ±4 kWh/m^2 and ±12 kWh/m^2 during 2020–2060 and 2061–2099, respectively, under the high-emission scenario, compared with that of 1990–2010. Although there is a slight decline in most regions of China, a relatively large increase is observed in the southeast of China, with a change rate of 18~30% [33], which is greater than the change rate in our study (6~10%). This might be because different data sources were used. Additionally, there is a significant increasing trend (5~10 W/m^2) in central and southeastern China, while decreases in northwestern China (5~15 W/m^2) and the Tibetan Plateau (5~10 W/m^2) are observed under the SSP585 scenario during the years of 2020–2100 [13], which is highly consistent with our research. However, the result of energy yields from PV in our study is different from the result of PV power by Niu et al. [13], which leads to the different changes. Additionally, it is found that under the high-emission scenario, the photovoltaic power output will decrease by −0.04%/year in western China and increase by 0.06~0.1%/year in southeastern China [34]; the solar PV power will increase in central and eastern China and decrease in solar energy-abundant regions [35], in which the trends of PV energy yields are consistent with our research. The present PV energy potential is 299.55 kWh/(m^2·year), which is slightly higher than 277.2 kWh/(m^2·year), found by Zhao et al. [36], and 276 kWh/(m^2·year), found by Liu et al. [37]. This is because in this study, the value of solar radiation on the tilted surface that is larger than the value of solar radiation on the horizontal surface was used to calculate the PV energy generation, which is more reasonable and closer to the reality. In this study, it is found that moderate climate change will enhance the PV energy generation, while strong or extreme warming will damage energy yield from photovoltaics, which is consistence with the study by Zhao et al. [18].

5. Conclusions

In summary, this study projected the PV energy yield in the near future (2020–2060) and far future (2061–2099) under the medium- and the high-emission scenarios, based on CMIP6 data. It seems that using the value of solar radiation on an inclined surface to simulate PV energy potential is more reasonable than using the value of solar radiation on a horizontal surface. There are significant results and conclusion that can be drawn as follows:

1. During the years of 2020–2099, under both emission scenarios, the overall trend of solar radiation in China increases. There are decreases in solar radiation in the northwest part of China, parts of the Tibetan Plateau, and Inner Mongolia. Increases

in solar radiation are observed in other regions of China, especially in southeastern and central China.

2. During the years of 2020–2099, under both scenarios, the temperature increases in northern China are greater than those in southern China. The largest temperature increase occurs under the SSP585 scenario during the years of 2061–2099. The increase in temperature becomes progressively more intense as time goes on and intensifies emissions.
3. In terms of China's PV energy potential, generally, under both scenarios, there is not much change, compared with that of the referenced period (1990–2010). However, there are imbalances in PV energy yield changes in different regions of China. Under both scenarios, generally, there are obvious increases in southeastern and central China, while decreases are observed in northwestern China, the Tibetan Plateau, and Inner Mongolia. This is mainly because the temperatures in these regions increase more and solar radiation increases less than that of southeastern and central China, and PV energy yield has direct positive and negative proportions to solar radiation and temperature, respectively.
4. According to the above results, it is demonstrated that under the medium-emission scenario, climate change could increase the PV energy potential, while under the high-emission scenario, it will inhibit PV energy potential during the years of 2020–2099. Thus, the Chinese government's carbon peaking and carbon neutrality goals will enhance the PV energy potential to some extent in the future. Meanwhile, there are some suggestions for China's solar photovoltaic development. Firstly, improving photovoltaic technology, especially by improving PV cell efficiency, should be encouraged, which may compensate for the effect of extreme global warming. Secondly, the site selection of PV installation will become more important in the future. Currently, 60% percent of PV farms are installed in northwestern China, Tibet, and Inner Mongolia, due to their abundance of solar radiation and the vast areas of the Gobi Desert. Thus, the future plan of solar photovoltaic deployment should pay more attention to southeastern and central China, due to their significant rise in PV energy potential in the future.

There are still limitations in this study. Although solar radiation on an inclined surface is applied to simulate PV energy potential, the other factors, such as wind velocity, cloud thickness, PV technology improvement, and so on, are not considered in this study, which might lead to inconsistencies with the actual situation. In the future, more factors will be included in the projection of the PV energy potential, and economic benefit analysis will be conducted in the context of climate change.

Author Contributions: Conceptualization and methodology, Y.H.; software, Y.G.; formal analysis, Y.H. and J.Y.; investigation, M.W. and W.H.; resources, Y.H. and M.W.; data curation, Y.H. and M.W.; writing—original draft preparation, Y.H.; writing—review and editing, Y.G. and L.C.; visualization, Y.G.; supervision, Y.G.; project administration, Y.H.; funding acquisition, Y.H. All authors have read and agreed to the published version of the manuscript.

Funding: This research was funded by the Natural Science Foundation of Gansu province (No. 21JR11RA213), Commissioner for Science and Technology of Gansu province (No. 23CXGA0063), and Innovation and Entrepreneurship Talent Project of Gansu Organization Department (No. 2021LQGR38), National Natural Science Foundation of China (No. 42301309).

Institutional Review Board Statement: Not applicable.

Informed Consent Statement: Not applicable.

Data Availability Statement: The data were obtained from ESGF (https://esgf-node.llnl.gov/search/cmip6/) (accessed on 20 May 2023) and China's Meteorological Administration (http://data.cma.cn) (accessed on 20 May 2023)).

Conflicts of Interest: The authors declare no conflicts of interest.

References

1. International Energy Agency (IEA). Snapshot of Global PV Markets 2023, Photovoltaic Power System Programme (PPSP). Available online: https://iea-pvps.org/wp-content/uploads/2023/04/IEA_PVPS_Snapshot_2023.pdf (accessed on 3 April 2023).
2. Wild, M.; Folini, D.; Henschel, F.; Fischer, N.; Müller, B. Projections of long-term changes in solar radiation based on CMIP5 climate models and their influence on energy yields of photovoltaic systems. *Sol. Energy* **2015**, *116*, 12–24. [CrossRef]
3. Crook, J.; Jones, L.; Forster, P.; Crook, R. Climate change impacts on future photovoltaic and concentrated solar power energy output. *Energy Environ. Sci.* **2011**, *4*, 3101–3109. [CrossRef]
4. Müller, B.; Wild, M.; Driesse, A.; Behrens, K. Rethinking solar resource assessments in the context of global dimming and brightening. *Sol. Energy* **2014**, *99*, 272–282. [CrossRef]
5. Wild, M.; Gilgen, H.; Roesch, A.; Ohmura, A.; Long, C.; Dutton, E.; Forgan, B.; Kallis, A.; Russak, V.; Tsvetkov, A. From Dimming to Brightening: Decadal Changes in Solar Radiation at Earth's Surface. *Science* **2005**, *308*, 847–850. [CrossRef] [PubMed]
6. Wild, M. Global dimming and brightening: A review. *J. Geophys. Res.* **2009**, *114*, D00D16. [CrossRef]
7. Jerez, S.; Tobin, I.; Vautard, R.; Montavez, J.; Lopez-Romero, J.; Thais, F.; Bartok, B.; Christensen, O.; Colette, A.; Deque, M.; et al. The impact of climate change on photovoltaic power generation in Europe. *Nat. Commun.* **2015**, *6*, 10014. [CrossRef] [PubMed]
8. Gaetani, M.; Huld, T.; Vignati, E.; Monforti-Ferrario, F.; Dosio, A.; Raes, F. The near future availability of photovoltaic energy in Europe and Africa in climate aerosol modeling experiments. *Renew. Sustain. Energy Rev.* **2014**, *38*, 706–716. [CrossRef]
9. Hou, X.; Wild, M.; Folini, D.; Kazadzis, S.; Wohland, J. Climate change impacts on solar power generation and its spatial variability in Europe based on CMIP6. *Earth Syst. Dynam.* **2021**, *12*, 1099–1113. [CrossRef]
10. Dutta, R.; Chanda, K.; Maity, R. Future of solar energy potential in a changing climate across the world: A CMIP6 multi-model ensemble analysis. *Renew. Energy* **2022**, *188*, 819–829. [CrossRef]
11. Danso, D.; Anquetin, S.; Diedhiou, A.; Lavaysse, C.; Hingray, B.; Raynaud, D.; Kobea, A. A CMIP6 assessment of the potential climate change impacts on solar photovoltaic energy and its atmospheric drivers in West Africa. *Environ. Res. Lett.* **2022**, *17*, 44016. [CrossRef]
12. Zuluaga, C.; Avila-Diaz, A.; Justino, F.; Martins, F.; Ceron, W. The climate change perspective of photovoltaic power potential in Brazil. *Renew. Energy.* **2022**, *193*, 1019–1031. [CrossRef]
13. Niu, J.; Wu, J.; Qin, W.; Wang, L.; Yang, C.; Zhang, M.; Zhang, Y.; Qi, Q. Projection of future carbon benefits by photovoltaic power potential in China using CMIP6 statistical downscaling data. *Environ. Res. Lett.* **2023**, *18*, 094013. [CrossRef]
14. Chen, X.; Zhou, C.; Tian, Z.; Mao, H.; Luo, Y.; Sun, D.; Fan, J.; Jiang, L.; Deng, J.; Rosen, M. Different photovoltaic power potential variations in East and West China. *Appl. Energy* **2023**, *351*, 121846. [CrossRef]
15. Zuo, H.; Lu, H.; Sun, P.; Qiu, J.; Li, F. Changes in photovoltaic power output variability due to climate change in China: A multi-model ensemble mean analysis. *J. Renew. Sustain. Energy* **2024**, *16*, 023503. [CrossRef]
16. Guo, J.; Chen, Z.; Meng, J.; Zheng, H.; Fan, Y.; Ji, L.; Wang, X.; Liang, X. Picturing China's photovoltaic energy future: Insights from CMIP6 climate projections. *Renew. Sustain. Energy Rev.* **2024**, *189*, 114026. [CrossRef]
17. Zhang, Y.; Gao, Y.; Xu, L.; Guan, X.; Gong, A.; Zhang, M. Assessment of future solar energy potential changes under the shared socio-economic pathways scenario 2–4.5 with WRF-chem: The roles of meteorology and emission. *Atmos. Environ.* **2023**, *318*, 120232. [CrossRef]
18. Müller, J.; Folini, D.; Wild, M.; Pfenninger, S. CMIP-5 models project photovoltaics are a no-regrets investment in Europe irrespective of climate change. *Energy* **2019**, *171*, 135–148. [CrossRef]
19. Lu, N.; Yao, L.; Qin, J.; Yang, K.; Wild, M.; Jiang, H. High emission scenario substantially damages China's photovoltaic potential. *Geophys. Res. Lett.* **2022**, *49*, e2022GL100068. [CrossRef]
20. Mark, Z.; Jacobson, V. World estimates of PV optimal tilt angles and ratios of sunlight incident upon tilted and tracked PV panels relative to horizontal panels. *Sol. Energy* **2018**, *169*, 55–66. [CrossRef]
21. Chang, T. The Sun's apparent position and the optimal tilt angle of a solar collector in the northern hemisphere. *Sol. Energy* **2009**, *83*, 1274–1284. [CrossRef]
22. Zhang, L.; Chen, X.; Xin, X. Short commentary on CMIP6 Scenario Model Intercomparison Project (ScenarioMIP). *Adv. Clim. Change Res.* **2019**, *15*, 519–525.
23. Ren, X.; He, H.; Zhang, L.; Yu, G. Global radiation, photosynthetically active radiation, and the diffuse components dataset of China, 1981–2010. *Earth Syst. Sci. Data* **2018**, *10*, 1217–1226. [CrossRef]
24. Liu, B.; Jordan, R. Daily insolation on surfaces tilted toward the equator. *ASHRAE Trans.* **1962**, *10*, 526–541. [CrossRef]
25. Hay, J. Calculating solar radiation for inclined surfaces: Practical approaches. *Renew. Energy* **1993**, *3*, 373–380. [CrossRef]
26. Hua, Y.; He, W.; Liu, P. Optimum tilt angles of solar panels: A case study for Gansu province, northwest China. *Appl. Sol. Energy* **2020**, *56*, 388–396.
27. Skoplaki, E.; Palyvos, J. On the temperature dependence of photovoltaic module electrical performance: A review of efficiency/power correlations. *Sol. Energy* **2009**, *83*, 614–624. [CrossRef]
28. Zondag, H. Flat-plate PV-Thermal collectors and systems: A review. *Renew. Sustain. Energy Rev.* **2008**, *12*, 891–959. [CrossRef]
29. Evans, D. Simplified method for predicting photovoltaic array output. *Sol. Energy* **1981**, *27*, 555–560. [CrossRef]
30. Lasiner, F. *Photovoltaic Engineering Handbook*; Higler, A., Ed.; Routledge: Princeton, NY, USA, 1990.
31. Klein, S. Calculation of monthly average insolation on tilted surfaces. *Sol. Energy* **1977**, *19*, 325–329. [CrossRef]

32. Zou, L.; Wang, L.; Li, J.; Lu, Y.; Gong, W.; Niu, Y. Global surface solar radiation and photovoltaic power from Coupled Model Intercomparison Project Phase 5 climate models. *J. Clean. Prod.* **2019**, *224*, 304–324. [CrossRef]
33. Zhao, X.; Huang, G.; Lu, C.; Zhou, X.; Li, Y. Impacts of climate change on photovoltaic energy potential: A case study of China. *Appl. Energ.* **2020**, *280*, 115888. [CrossRef]
34. Yang, L.; Jiang, J.; Liu, T.; Li, Y.; Zhou, Y.; Gao, X. Projections of future changes in solar radiation in China based on CMIP5 climate models. *Glob. Energy Interconnect.* **2018**, *1*, 452–459. [CrossRef]
35. Wu, J.; Han, Z.; Yan, Y.; Gao, X. Future projection of solar energy over China based on multi-regional climate model simulations. *Earth Space Sci.* **2022**, *9*, e2021EA002207. [CrossRef]
36. Zhao, X.; Yue, X.; Tian, C.; Zhou, H.; Wang, B.; Chen, Y.; Zhao, Y.; Fu, W.; Hu, Y. Multimodel ensemble projection of photovoltaic power potential in China by the 2060s. *Atmos. Ocean. Sci. Lett.* **2023**, *16*, 100403. [CrossRef]
37. Liu, F.; Wang, X.; Sun, F.; Wang, H. Correct and remap solar radiation and photovoltaic power in China based on machine learning models. *Appl. Energy* **2022**, *312*, 118775. [CrossRef]